

Generalized Skyrme Crystals

J. Silva Lobo^{a,*}, R. S. Ward^a

^a*Department of Mathematical Sciences, Durham University, South Road, Durham, DH1 3LE, United Kingdom*

Abstract

This letter deals with triply-periodic (crystalline) solutions in a family of Skyrme systems, namely where the field takes values in the squashed 3-sphere. The family includes the standard Skyrme model (round 3-sphere), and the Skyrme-Faddeev case (maximal squashing). In the round case, the lowest-energy crystal is the well-known cubic lattice of half-skyrmions; but in the squashed case the minimal-energy crystal structures turn out to be different. We describe some of the solutions that arise, including arrays of vortices and multi-sheeted structures.

Keywords: Skyrmons, hopf solitons

1. Introduction

In the basic SU(2) Skyrme model, the solution with the lowest energy-per-charge E_N is the triply-periodic skyrme crystal [1]. For a given value of the topological charge (winding number, or baryon number) N , there are in general many isolated N -skyrmion solutions, i.e. local minima of the energy; but the belief is that for $N \gg 1$, the lowest-energy solution will resemble a chunk of the skyrme crystal.

However, in the Skyrme-Faddeev system, where the field takes values in S^2 and the topological charge N is the Hopf number, the situation is less clear. If there were a triply-periodic crystalline solution with $E_N = c$ (where c is a constant independent of N), as in the Skyrme case, then a large crystalline chunk would have $E_N \sim c$. But we know [2] that there exist solutions with $E_N \sim N^{-1/4}$, so such a crystal chunk certainly could not be the global energy minimum among fields of charge N , although it could be a local minimum. In general, it seems to be the case that Hopf solitons tend to clump into a tangle; various examples, for low values of N , may be seen in [3, 4, 5, 6, 7].

The aim of this letter is to explore this difference in behaviour, by investigating triply-periodic crystalline solutions in a system which interpolates between the two cases above. This generalized Skyrme system was introduced in [8]; it is labelled by a parameter $\alpha \in [0, 1]$, in such a way that $\alpha = 0$ gives the ‘pure’ Skyrme model, whereas $\alpha = 1$ gives the Skyrme-Faddeev model. In particular, we wish to see what happens to the skyrme crystal as the system deforms away from the basic Skyrme case.

The interpolating system is very natural geometrically. For simplicity, let us restrict to static fields in all of what

follows. Let Σ be a compact 3-dimensional, oriented, connected Riemannian manifold. Then for fields $\Phi : \mathbb{R}^3 \rightarrow \Sigma$, the Skyrme energy functional $E[\Phi]$ has a natural definition, depending in particular on the metric of Σ [9]. With the usual boundary condition $\Phi(x^j) \rightarrow \Phi_0$ as $|x^j| \rightarrow \infty$, where Φ_0 is some specified point on Σ , the topological charge N is defined to be the degree of the map Φ . Our system is obtained by taking Σ to be the squashed 3-sphere (Berger sphere): the standard 3-sphere squashed along its Hopf fibres by a factor $1 - \alpha$. If $\alpha = 0$, there is no squashing: the target space is just the round sphere SU(2), and we have the Skyrme model. In the degenerate case $\alpha = 1$, the 3-sphere becomes a 2-sphere, the winding number N becomes the Hopf number, and we have the Skyrme-Faddeev model.

The system has a potential condensed-matter interpretation in which the two complex fields (Z_1, Z_2) represent two flavours of Cooper pairs [10]. The parameter α then appears as the coefficient of a term $J_\mu J^\mu$, where $J_\mu = iZ^\dagger \partial_\mu Z$ is the current density. In particular, arrays might be of interest in this context.

2. The Generalized Skyrme System

In this section, we give some details of the one-parameter interpolating family of Skyrme systems. The field is denoted $\Phi_\beta = (\Phi_1, \Phi_2, \Phi_3, \Phi_4)$, where each component Φ_β is a function of the spatial coordinates $x^j = (x^1, x^2, x^3) = (x, y, z)$, and the constraint $\Phi_\beta \Phi_\beta = 1$ is imposed. The energy density for the system, parametrized by $\alpha \in [0, 1]$, is

$$\mathcal{E} = \lambda_2 [(\partial_j \Phi_\beta)(\partial_j \Phi_\beta) - \alpha P_j P_j] + \lambda_4 [2(1 - \alpha) F_{\beta\gamma}^j F_{\beta\gamma}^j + \alpha Q^j Q^j], \quad (1)$$

*Corresponding author

Email addresses: j.i.silva-lobo@durham.ac.uk (J. Silva Lobo), richard.ward@durham.ac.uk (R. S. Ward)

where

$$\begin{aligned} P_j &= \Omega_{\beta\gamma} \Phi_\beta \partial_j \Phi_\gamma, \\ F_{\beta\gamma}^j &= \frac{1}{2} \varepsilon^{jkl} (\partial_k \Phi_\beta) (\partial_l \Phi_\gamma), \\ Q^j &= \Omega_{\beta\gamma} F_{\beta\gamma}^j, \end{aligned}$$

with $\Omega_{\beta\gamma}$ being a symplectic form with non-zero components $\Omega_{12} = -\Omega_{21} = -\Omega_{34} = \Omega_{43} = 1$. The coupling constants λ_2 and λ_4 can be scaled as desired, by changing the units of energy and length; in what follows, we shall use the ‘geometrical’ choice $\lambda_2 = 1/[4\pi^2(3 - \alpha)]$ and $\lambda_4 = 1/[4\pi^2(3 - 2\alpha)]$ as in [8]. The effect of this is that the energy of a 1-skyrmion on \mathbb{R}^3 is approximately independent of α ($E_1 \approx 1.22$).

If we are thinking of the Skyrme model as a nonlinear theory of pions, then the deformation when α becomes positive may be viewed as putting one of the three pions on a different footing from the other two. To see this explicitly, we impose the boundary condition $\Phi_\mu \rightarrow (0, 0, 0, 1)$ as $|x^j| \rightarrow \infty$, and identify (Φ_1, Φ_2, Φ_3) as the pion fields in the usual way. Then in the asymptotic region the energy density (1) becomes

$$\mathcal{E} \approx \lambda_2 [(\partial_j \Phi_1)^2 + (\partial_j \Phi_2)^2 + (1 - \alpha)(\partial_j \Phi_3)^2]. \quad (2)$$

If $\alpha = 1$, then one of the fields becomes non-dynamic. This amounts to passing from the original target space $S^3 \cong \text{SU}(2)$ to the quotient space $S^2 \cong \text{SU}(2)/\text{U}(1)$, by the Hopf projection

$$\begin{aligned} \psi_1 &= 2(\Phi_1 \Phi_3 - \Phi_2 \Phi_4), \\ \psi_2 &= 2(\Phi_2 \Phi_3 + \Phi_1 \Phi_4), \\ \psi_3 &= \Phi_3^4 + \Phi_4^2 - \Phi_1^2 - \Phi_2^2. \end{aligned} \quad (3)$$

The relevant field is then the unit 3-vector $\vec{\psi}$, and the energy density (1) becomes

$$\mathcal{E} = \frac{1}{32\pi^2} \left[(\partial_j \vec{\psi})^2 + \frac{1}{4} (G_{jk})^2 \right], \quad (4)$$

where $G_{jk} = \vec{\psi} \cdot (\partial_j \vec{\psi}) \times (\partial_k \vec{\psi})$. This is the Skyrme-Faddeev energy [11].

The energy $E[\Phi]$ is the integral of (1) over \mathbb{R}^3 , or over a fundamental cell if one is dealing with periodic fields. There is a Bogomolny-type lower bound [9] on the energy of fields with topological charge N , namely $E \geq 6N\sqrt{\lambda_2\lambda_4} \text{vol}(\Sigma)$. Using the fact that the volume of the squashed 3-sphere is $2\pi^2\sqrt{1 - \alpha}$, and with our choice of λ_2 and λ_4 , this gives

$$E_N \geq \frac{\sqrt{1 - \alpha}}{\sqrt{(1 - \alpha/3)(1 - 2\alpha/3)}}. \quad (5)$$

In the limit $\alpha = 1$, the bound (5) becomes trivial. There are various nontrivial bounds in this case. For isolated Hopf solitons on \mathbb{R}^3 , we know that $E_N \geq cN^{-1/4}$, where c is a constant; it is conjectured that this bound

holds for $c = 1$ [12]. This bound is not valid for triply-periodic fields $\Phi : T^3 \rightarrow S^2$; but in that case there is another lower bound, which follows from the general formula given in [13]: if Φ is triply-periodic, and L is the largest of its periods, then its normalized energy satisfies $E_N \geq \pi/(2L)$.

For $\alpha = 0$, the expression (1) gives the standard static Skyrme energy, and it has an obvious $\text{O}(4)$ symmetry. For $\alpha \neq 0$, the symmetry is broken to $\text{U}(2)$, this being the subgroup of $\text{O}(4)$ which preserves the symplectic form Ω .

In this letter, we are focusing on crystalline configurations, so the fields are periodic in (x^1, x^2, x^3) with periods (L_1, L_2, L_3) respectively. In effect, Φ is a map from T^3 to S^3 , and it is classified topologically by its degree $N \in \mathbb{Z}$. The topological classification of maps from T^3 to S^2 , which is relevant to the $\alpha = 1$ case, is more complicated. But if we restrict to fields which are algebraically inessential, meaning that the 2-form G_{jk} belongs to the trivial cohomology class in $H^2(T^3, \mathbb{Z})$, then the classification remains a single integer $N \in \mathbb{Z}$ (cf. [14]). The Hopf charge of the Hopf projection $\vec{\psi}$ of Φ is equal to the degree of Φ , so it is consistent to let N denote either.

3. Crystals in the Generalized Skyrme Family

In this section, we investigate various triply-periodic solutions in the family of generalized Skyrme systems parametrized by α . There are many of these, corresponding to different local minima of the energy, and we shall describe only some of them.

The results that follow are obtained by numerical minimization of the energy functional $E[\Phi]$. More specifically, the expression for the energy is replaced by a second-order finite-difference approximation on a rectangular lattice with periodic boundary conditions, and the minima are found by conjugate-gradient relaxation. Testing with various different values of the lattice spacing indicates that the accuracy, for example in the energy E , is better than 1%. As remarked above, there are many local minima, and the initial configuration determines which one of these is obtained after flowing down the energy gradient. We also vary the side-lengths L_1 , L_2 and L_3 of the fundamental cell, so as to get the lowest possible value of $E[\Phi]$.

In the original Skyrme system ($\alpha = 0$), the lowest-energy crystal is a cubic lattice [1]. Its unit cell contains eight half-skyrmions, and has $N = 4$. We begin by taking this as the initial configuration, and minimizing $E[\Phi]$ for various values of α .

In the $\alpha = 0$ case, the minimum occurs at $L_1 = L_2 = L_3 = 4.7$; but the side-lengths cease to be all equal when $\alpha > 0$. This occurs because the system has less symmetry than when $\alpha = 0$; in particular, one of the spatial directions, which we take to be the x^3 -direction, is now on a different footing from the other two. For $\alpha > 0$, the half-skyrmions become elongated in the x^3 -direction, and the optimal side-lengths satisfy $L_1 = L_2 > L_3$. These aspects

are illustrated in Figure 1. The upper-left plot shows the optimal (minimal-energy) values of $L_1 = L_2$ and L_3 , as functions of α , in the range $0 \leq \alpha \leq 0.9$. We see that in

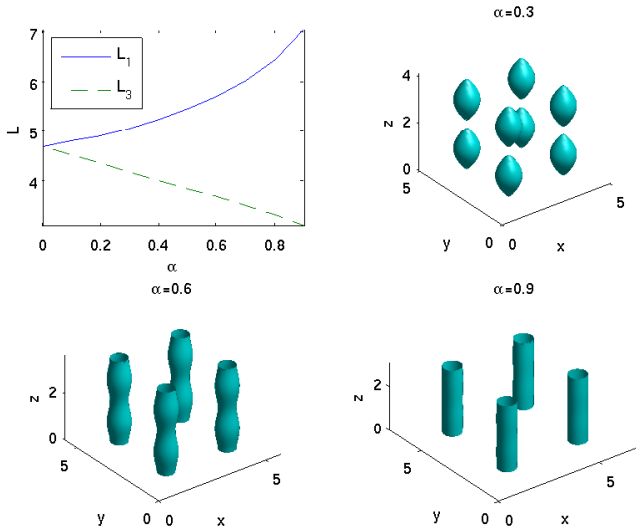


Figure 1: The V+AV+V+AV solution. Optimal values of $L_1 = L_2$, and L_3 ; and the energy density for $\alpha = 0.3, 0.6, 0.9$.

the Skyrme case $\alpha = 0$, we have $L_1 = L_2 = L_3 = 4.7$, as noted above; but as α increases, the lattice cells are compressed in the x^3 -direction and expanded in the x^1 - and x^2 -directions. The behaviour in the $\alpha = 1$ limit will be discussed in more detail below. The other three pictures in Figure 1 plot the energy density \mathcal{E} , or more precisely the surfaces where \mathcal{E} equals 0.7 times its maximum value, for three values of α ranging from 0.3 to 0.9. We see that as α increases, the half-skyrmions join up pairwise in the x^3 -direction, to form four parallel vortices; these are in fact two vortices and two antivortices, and so this field is called the V+AV+V+AV solution. In the $\alpha \rightarrow 1$ limit, the vortices become homogeneous in the x^3 -direction; such vortices will be discussed in more detail below.

The symmetries of the $\alpha > 0$ fields depicted in Figure 1 are a subset of the $\alpha = 0$ skyrme-crystal symmetries [1], and are generated by

$$x^j \mapsto L_j - x^j, \quad \Phi_4 \mapsto -\Phi_4 \quad \text{for } j = 1, 2, 3; \quad (6)$$

$$x^j \mapsto L_j/2 - x^j, \quad \Phi_j \mapsto -\Phi_j \quad \text{for } j = 1, 2, 3; \quad (7)$$

$$\begin{aligned} (x^1, x^2, x^3) &\mapsto (x^2, -x^1, x^3), \\ (\Phi_1, \Phi_2, \Phi_3, \Phi_4) &\mapsto (\Phi_2, \Phi_1, \Phi_3, -\Phi_4). \end{aligned} \quad (8)$$

The normalized energy of these solutions is plotted in Figure 2, as a function of α . The other plots in Figure 2 are the Bogomolny bound (5), and the energies of two other triply-periodic solutions which will be described below.

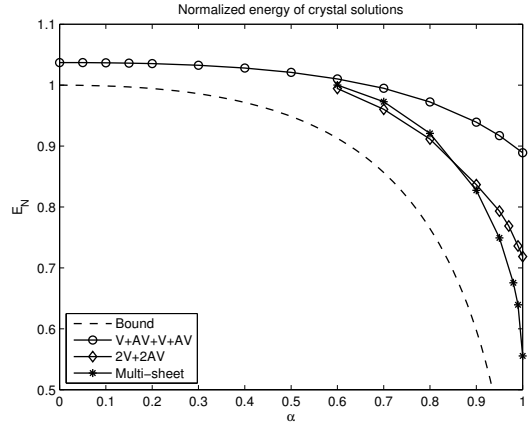


Figure 2: Normalized energy E_N of crystalline solutions, versus α .

At this point, let us say more about x^3 -homogeneous vortices. The field of a p -vortex with unit x^3 -twist, located on the x^3 -axis, can be put in the form

$$\Phi_1 + i\Phi_2 \approx (x^1 + ix^2)^p, \quad \Phi_3 + i\Phi_4 \approx \exp(2\pi i x^3/L_3) \quad (9)$$

near that axis. If $p > 0$, we refer to it as a p -vortex, whereas if $p < 0$ we refer to it as a p -antivortex. If we restrict the Hopf projection ψ of Φ to the plane $x^3 = 0$, we get a map from T^2 to S^2 ; the degree of this map is the total vortex number in the x^3 -direction (taking the multiplicity p of each vortex into account). This total vortex number has to be zero, since it is the degree of a Hopf projection. In other words, there have to be an equal number of vortices and antivortices. The topological charge N is the sum of the absolute values of the vortex numbers; in other words, vortices and antivortices both contribute positively to N . The $\alpha = 0.9$ field illustrated in Figure 1 is close to an $N = 4$ multi-vortex configuration, with two 1-vortices and two 1-antivortices, and hence is referred to as V+AV+V+AV.

It is worth noting that analogous V+AV+V+AV configurations can appear in the $\alpha = 0$ case, for values of the side-lengths L_j which differ from the optimal ones [15].

Skyrme vortices, or more precisely vortex-antivortex pairs, were discussed in [16]. In particular, it was shown there that if one has a parallel vortex-antivortex pair separated by a (large) distance D , then there is an attractive force between them, the leading term of which is proportional to $1/D$. In our α -family, the expression for the attractive force is the same, except that it acquires a factor of $1 - \alpha$. In other words, vortices and antivortices attract one another, as long as $\alpha < 1$. In the $\alpha \rightarrow 1$ limit, however, the leading-order term vanishes. It is not known whether there is still an attractive vortex-antivortex force in this limit, but numerical experiments suggest that the force becomes repulsive. In particular, the two vortices and two antivortices in our picture repel each other when $\alpha = 1$, and therefore $L_1, L_2 \rightarrow \infty$ as $\alpha \rightarrow 1$, consistent with the upper-left plot in Figure 1.

The second vortex-type solution featuring in Figure 2

is $2V+2AV$, and it consists of a 2-vortex and a parallel 2-antivortex. Its energy is plotted for $\alpha \geq 0.6$, and it is apparent that in this range, its energy is less than that of $V+AV+V+AV$. In this case, the numerical evidence again suggests that $L_1, L_2 \rightarrow \infty$ as $\alpha \rightarrow 1$, implying that the 2-vortex and the 2-antivortex repel each other in that limit. The four pictures in Figure 3 plot the energy density isosurfaces where \mathcal{E} equals 0.8 times its maximum value, for four values of α ranging from 0.6 to 0.99.

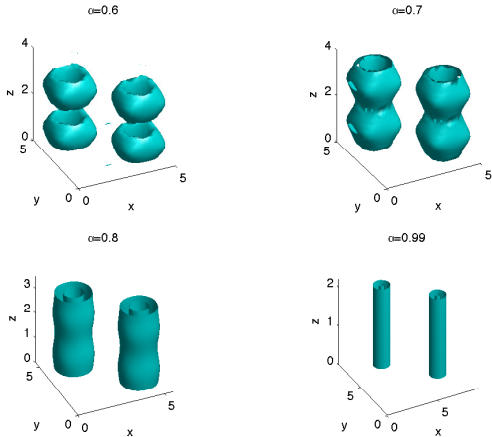


Figure 3: The $2V+2AV$ solution: energy densities for $\alpha = 0.6, 0.7, 0.8, 0.99$.

Note that in the $\alpha = 1$ (Skyrme-Faddeev) system, we can have vortices without antivortex partners — the restriction of the net vortex number being zero does not apply in this case. Such Hopf-vortex fields have been the subject of several studies, such as [17, 5, 7]. The results described above suggest that in the Skyrme-Faddeev system, the normalized energy of a p -vortex decreases as p increases. This indeed turns out to be the case, as we now explain in more detail.

Consider fields $\vec{\psi}$ with energy density (4) on $\mathbb{R}^2 \times S^1$. So $\vec{\psi}$ is periodic in x^3 with period L , and it satisfies the boundary condition $\vec{\psi} \rightarrow (0, 0, 1)$ as $\rho \rightarrow \infty$, where $x^1 + ix^2 = \rho e^{i\theta}$. More specifically, consider rotationally-symmetric p -vortices centred on the x^3 -axis: these will have the form

$$\psi_1 + i\psi_2 = \sin(f) \exp(ip\theta + 2\pi i x^3/L), \quad \psi_3 = \cos(f), \quad (10)$$

where $f = f(\rho)$ satisfies $f(0) = \pi$ and $f(\rho) \rightarrow 0$ as $\rho \rightarrow \infty$. Finding the minimal energy $E(p)$ for various values of the vortex number p is a straightforward numerical computation, and this was done for $p = 1, \dots, 5$. Let us, as usual, normalize the energy $E(p)$ by dividing it by the topological charge p . The result is that $E(p)$ depends linearly on $1/p$:

$$E(p) \approx 0.338/p + 0.551;$$

and it is this value (with, respectively, $p = 1$ and $p = 2$) which is used for the $\alpha = 1$ ends of the $V+AV+V+AV$ and $2V+2AV$ plots in Figure 2.

In view of the above, it seems likely that triply-periodic solutions with even lower values of E_N than $V+AV+V+AV$ and $2V+2AV$ could be constructed by assembling parallel arrays of p -vortices and p -antivortices for $p \geq 3$; but this has not been investigated further.

The solutions corresponding to the final plot in Figure 2, referred to as “multi-sheet”, have a lower value of energy-per-charge than the others mentioned previously if $\alpha \geq 0.9$, and do not resemble parallel vortex-antivortex configurations for α close to 1. Figure 4 shows the energy density isosurfaces where \mathcal{E} equals 0.8 times its maximum value, for four values of α ranging from 0.6 to 0.99. As

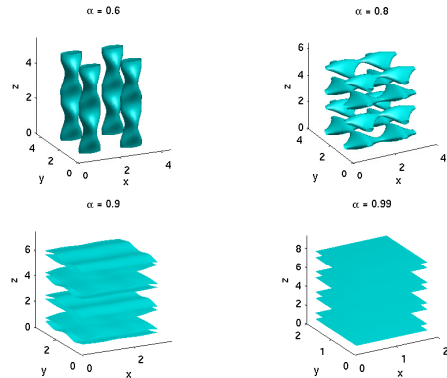


Figure 4: The “multi-sheet” solution: energy densities for $\alpha = 0.6, 0.8, 0.9, 0.99$.

α approaches 1, they are closely approximated by fields which are homogeneous in x^1 and x^2 , in fact of the form

$$Z_1 := \Phi_1 + i\Phi_2 = \sin(f) \exp(2\pi i \varepsilon_2 x^2/L_2), \quad (11)$$

$$Z_2 := \Phi_4 + i\Phi_3 = \cos(f) \exp(2\pi i \varepsilon_1 x^1/L_1), \quad (12)$$

where $\varepsilon_1 = \pm 1$, $\varepsilon_2 = \pm 1$, and $f = f(x^3)$. Their energy density depends only on x^3 , and is peaked on sheets orthogonal to the x^3 -axis. Such fields arise if we impose the symmetries generated by

$$x^1 \mapsto x^1 + c, \quad (Z_1, Z_2) \mapsto (Z_1, Z_2 \exp(2\pi i \varepsilon_1 c/L_1)); \quad (13)$$

$$x^2 \mapsto x^2 + c, \quad (Z_1, Z_2) \mapsto (Z_1 \exp(2\pi i \varepsilon_2 c/L_2), Z_2); \quad (14)$$

$$(x^1, x^2) \mapsto (-x^1, -x^2), \quad (Z_1, Z_2) \mapsto (\overline{Z_1}, \overline{Z_2}). \quad (15)$$

Note that such transformations on (Z_1, Z_2) preserve the energy (1). In other words, translations in x^1 or x^2 , and an inversion, can be compensated by a symmetry transformation of the field.

In order to have periodicity in x^3 , and for the topological charge N to be nonzero, we need to arrange things rather carefully. A periodic field with $N = 4$ is obtained by imposing $f(kL_3/4) = k\pi/2$ for $k = 0, 1, 2, 3, 4$, and

$$(\varepsilon_1, \varepsilon_2) = \begin{cases} (1, 1) & \text{for } 0 \leq x^3 < L_3/4, \\ (-1, 1) & \text{for } L_3/4 \leq x^3 < L_3/2, \\ (-1, -1) & \text{for } L_3/2 \leq x^3 < 3L_3/4, \\ (1, -1) & \text{for } 3L_3/4 \leq x^3 < L_3. \end{cases}$$

Note that the resulting field is continuous.

Substituting (11, 12) into the formula (1) for the energy density gives an expression of the form $\mathcal{E} = A(f) (f')^2 + B(f)$, where $f' = df/dx^3$. Then a standard Bogomolny argument implies that, for given values of L_1 and L_2 (and α), the normalized energy E attains a minimum value

$$E(\alpha, L_1, L_2) = 2L_1L_2 \int_0^{\pi/2} \sqrt{AB} df, \quad (16)$$

when L_3 is given by

$$L_3 = 4 \int_0^{\pi/2} \sqrt{A/B} df. \quad (17)$$

The next step is to minimize (16) with respect to L_1 and L_2 , which was done using numerical integration. The resulting minimal energy for the ansatz (11, 12) approaches that of the multi-sheet solution (which is not quite homogeneous in x^1 and x^2) as $\alpha \rightarrow 1$. For example, if $\alpha = 0.98$, then the ansatz energy (16) is only 0.6% higher than that of the actual multi-sheet solution, and the fields are almost identical.

For $\alpha \geq 0.9$, the multi-sheet solution has the lowest energy-per-charge of those that we investigated. However, the $\alpha \rightarrow 1$ limit of this solution, and of the ansatz, is rather pathological, since the optimal values of $L_1 = L_2$ tend to zero. In fact, the energy (16) equals

$$E = 2\pi \int_0^{\pi/2} \sqrt{2\lambda_2^2 \sin^2(2f)L_1^2 + 4\pi^2\lambda_2\lambda_4 \sin^4(2f)} df \quad (18)$$

when $\alpha = 1$ (and where we have put $L_1 = L_2$), from which it is clear that its minimal value is attained when $L_1 = 0$. At first sight, this behaviour may seem paradoxical, since the usual view is that the fourth-order Skyrme term in the energy prevents an object with nontrivial 3-dimensional topology from shrinking to zero volume. This view is indeed correct for $0 \leq \alpha < 1$: in particular, if α lies in this range, then a triply-periodic configuration with nonzero topological charge N has an energy which diverges if any of its periods tends to zero. But in the $\alpha = 1$ limit, namely for the Skyrme-Faddeev system, this property no longer holds. One can see directly from (11, 12), or rather its Hopf projection, why this is so. If one scales each of the periods L_j , then each term in the expression of the energy of $\vec{\psi}$ scales differently. In particular, the term $\int (G_{12})^2$ has the form

$$\int (G_{12})^2 dx^1 dx^2 dx^3 = K \frac{L_3}{L_1 L_2},$$

where K is its value when $L_1 = L_2 = L_3 = 1$. This is the only term which prevents L_1 and L_2 from going to zero simultaneously. But for (11, 12) the quantity G_{12} is identically zero, and consequently one can always lower the energy by reducing L_1 and L_2 .

4. Conclusions

We have studied triply-periodic stable solutions (local minima of the energy) in a family of Skyrme-type systems parametrized by $\alpha \in [0, 1]$, which interpolates between the standard Skyrme model (at $\alpha = 0$) and the Skyrme-Faddeev system (at $\alpha = 1$). At $\alpha = 0$, the lowest-energy crystal resembles a cubic lattice of half-skyrmion particles, and this picture persists near $\alpha = 0$, as one would expect. But for larger values of α , various other configurations are preferred (that is, have lower energy-per-charge): for example, vortex-antivortex arrays and multi-sheet structures.

All these structures are somewhat problematic in the $\alpha \rightarrow 1$ limit, and it remains unclear whether or not there exists a smooth Skyrme-Faddeev crystal which is at least stable under small perturbations. As remarked in the introduction, the sublinear behaviour of the energy perhaps makes this unlikely. But the possibility remains open, and is worth further investigation.

Acknowledgments. Support from the UK Engineering and Physical Sciences Research Council (under grant EP/G038775/1), and the UK Science and Technology Facilities Council (under ST/G000433/1), is gratefully acknowledged.

References

- [1] N S Manton and P M Sutcliffe, *Topological Solitons*, Cambridge University Press, Cambridge, 2004.
- [2] F Lin and Y Yang, Existence of energy minimizers as stable knotted solitons in the Faddeev model. *Commun Math Phys* **249** (2004) 273–303.
- [3] R A Battye and P M Sutcliffe, Solitons, Links and Knots. *Proc Roy Soc Lond A* **455** (1999) 4305–4331.
- [4] J Hietarinta and P Salo, Faddeev-Hopf knots: dynamics of linked un-knots. *Phys Lett B* **451** (1999) 60–67.
- [5] J Hietarinta, J Jäykkä and P Salo, Relaxation of twisted vortices in the Faddeev-Skyrme model. *Phys Lett A* **321** (2004) 324–329.
- [6] P M Sutcliffe, Knots in the Skyrme-Faddeev model. *Proc Roy Soc Lond A* **463** (2007) 3001–3020.
- [7] J Jäykkä and J Hietarinta, Unwinding in Hopfion vortex bunches. arXiv:0904.1305
- [8] R S Ward, Skyrmsions and Faddeev-Hopf solitons. *Phys Rev D* **70** (2004) 061701.
- [9] N S Manton, Geometry of Skyrmsions. *Commun Math Phys* **111** (1987) 469–478.
- [10] E Babaev, L Faddeev and A J Niemi, Hidden symmetry and duality in a charged two-condensate Bose system. *Phys Rev B* **65** (2002) 100512.
- [11] L Faddeev and A J Niemi, Stable knot-like structures in classical field theory. *Nature* **387** (1997) 58–61.
- [12] R S Ward, Hopf solitons on S^3 and \mathbf{R}^3 . *Nonlinearity* **12** (1999) 241–246.
- [13] J M Speight, Supercurrent coupling in the Faddeev-Skyrme model. *J Geom Phys* **60** (2010) 599–610.
- [14] S Krusch and J M Speight, fermionic quantization of Hopf solitons. *Commun Math Phys* **264** (2006) 391–410.
- [15] J Silva Lobo, Deformed Skyrme Crystals. *JHEP* **10** (2010) 029.
- [16] D Harland and R S Ward, Chains of skyrmions. *JHEP* **12** (2008) 093.
- [17] M Miettinen, A J Niemi and Y Stroganov, Aspects of duality and confining strings. *Phys Lett B* **474** (2000) 303–308.